


# Acute effects of static stretching on skeletal muscle relaxation at different ankle joint angles

Stefano Longo<sup>1</sup>  · Michela Devoto<sup>1</sup> · Elena Monti<sup>1</sup> · Massimo Venturelli<sup>1</sup> · Eloisa Limonta<sup>1</sup> · Susanna Rampichini<sup>1</sup> · Angela Valentina Bisconti<sup>1</sup> · Fabio Esposito<sup>1</sup> · Emiliano Cè<sup>1</sup>

Received: 28 June 2016 / Accepted: 10 August 2016 / Published online: 18 August 2016  
© Springer-Verlag Italia 2016

## Abstract

**Purpose** By combining electromyographic (EMG), mechanomyographic (MMG) and force analysis, the electromechanical delay during muscle relaxation (R-Delay<sub>TOT</sub>) was partitioned into electrochemical and mechanical components. The study aimed to evaluate the effects of changes in joint angle on R-Delay<sub>TOT</sub> components during relaxation after electrically evoked contractions before and after static stretching (SS) administration. **Methods** Nineteen male participants (age  $24 \pm 3$  years; body mass  $76.4 \pm 8.9$  kg; stature  $1.78 \pm 0.09$  m; mean  $\pm$  SD) were evaluated. Passive torque ( $T_{pass}$ ) of the plantarflexor muscles was measured at  $0^\circ$ ,  $10^\circ$ , and  $20^\circ$  of dorsiflexion to determine joint stiffness. The maximum electrically evoked torque (pT) was also recorded at each angle. During pT, force, EMG and MMG signals were detected for offline calculations of R-Delay<sub>TOT</sub> and its electrochemical and mechanical components. The same procedures were repeated after SS.

**Results** With increase in dorsiflexion angle, joint stiffness increased while R-Delay<sub>TOT</sub> and its mainly mechanical components decreased (from  $-8$  to  $20$  %,  $P < 0.05$ ). After SS, joint stiffness decreased (from  $16$  to  $20$  %,  $P < 0.05$ ), while R-Delay<sub>TOT</sub> and its mainly mechanical components lengthened (from  $8$  to  $28.5$  %,  $P < 0.05$ ). Moreover, post-SS R-Delay<sub>TOT</sub> and its components decreased with the increase in joint angle (from  $-13$  to  $31$  %,  $P < 0.05$ ).

**Conclusion** The reduction in R-Delay<sub>TOT</sub> with increase in joint angle could be ascribed to the increase in joint stiffness, and not to alterations of the electrochemical processes during relaxation. SS lengthened R-Delay<sub>TOT</sub> and its components with a concomitant decrease in joint stiffness. Nevertheless, the reduction of the R-Delay<sub>TOT</sub> mainly mechanical components seen with dorsiflexion was similar to that before SS.

**Keywords** Mechanomyogram · Joint stiffness · Passive force · Muscle elongation

## Abbreviations

EMG	Electromyogram
GM	Gastrocnemius medialis
MF	Mean frequency
MMG	Mechanomyogram
pT	Peak torque
R-Delay <sub>TOT</sub>	Total relaxation delay
R- $\Delta$ t	Time delay between force decay beginning and the largest MMG signal displacement during relaxation
F-MMG <sub>p-p</sub>	Time delay between the largest MMG displacement and force cessation
R- $\Delta$ t	Duration of peak-to-peak of the largest MMG signal displacement during relaxation
MMG <sub>p-p</sub>	Time delay between muscle electrical activation cessation and the beginning of force decay
R- $\Delta$ t	Root mean square
EMG-F	Range of motion
RMS	Series elastic components
ROM	Static stretching
SEC	Passive torque
SS	
$T_{pass}$	

✉ Stefano Longo  
stefano.longo@unimi.it

<sup>1</sup> Department of Biomedical Sciences for Health (SCIBIS),  
Università degli Studi di Milano, Via G. Colombo 71,  
20133 Milan, Italy

## Introduction

Muscle relaxation is a physiological phenomenon involving events that are electrochemical and mechanical in nature, from cessation of neuromuscular activation to the return of series elastic components (SEC) to their pre-contraction status [1–6]. During relaxation, there is a latency between the cessation of muscle electrical activity and the beginning of force decay [1], termed relaxation electromechanical delay [4]. Recently, a combined analysis of electromyographic (EMG), mechanomyographic (MMG), and force signals during muscle relaxation after voluntary [7, 8] and electrically evoked contractions [8, 9] allowed partitioning of total delay during relaxation ( $R\text{-Delay}_{\text{TOT}}$ ) into different components, thus providing insights into the relative duration of the electrochemical and mechanical processes involved [10]. At the end of a contraction, four delays can be calculated after the identification of specific markers on EMG, MMG, and force signals. The single components and the presumed underlying physiological events are: (1)  $R\text{-}\Delta t$  EMG-F (from the end of EMG signal to the beginning of force decay) spans from the beginning of  $\text{Ca}^{2+}$  re-uptake in the sarcoplasmic reticulum to the transition of cross-bridges from force-generating to non-force-generating status; (2)  $R\text{-}\Delta t$  F-MMG<sub>p-p</sub> (from initial force decay to the beginning of the largest MMG displacement) comprises the beginning of the rapid change in sarcomere length and the increase in detachment rate of cross-bridges; (3)  $R\text{-}\Delta t$  MMG<sub>p-p</sub> (the largest MMG displacement duration) incorporates the main phase of the detachment of cross-bridges and SEC relaxation; and (4)  $R\text{-}\Delta t$  MMG-F<sub>end</sub> (from the end of the largest MMG displacement to the return to baseline of force signal) constitutes the final return of cross-bridges and SEC to their pre-contraction status [7, 9]. The first  $R\text{-Delay}_{\text{TOT}}$  component is mainly electrochemical ( $R\text{-}\Delta t$  EMG-F) and the three successive components ( $R\text{-}\Delta t$  F-MMG<sub>p-p</sub>,  $R\text{-}\Delta t$  MMG<sub>p-p</sub>, and  $R\text{-}\Delta t$  MMG-F<sub>end</sub>) are mostly mechanical. However, it should be taken into account that this approach cannot identify perfectly the endpoint of the electrochemical mechanisms and the starting point of the mechanical events. Nonetheless, this approach requires light, portable and less expensive instrumentation.

During muscle contraction and relaxation, high level of reliability and sensitivity were reported for all components under different experimental models, among which peripheral fatigue [7, 9, 11, 12], muscle temperature manipulation [13], muscle elongation [14], contraction intensity [13], and joint angles variation [15]. In particular, the joint angle variation (i.e. length of the muscle–tendon unit) has been demonstrated to influence the mechanical

components of electromechanical delays during muscle contraction [15, 16]. Indeed, the shorter the muscle-tendon length, the longer the total electromechanical delay. When partitioning the electromechanical delay during contraction in electrochemical and mechanical components, only the latter was influenced by joint angle variations [15, 16]. This finding was explained by the presence of slack at short muscle–tendon length, which would prolong the time for the mechanical force transmission. However, whether the slack would also influence the dynamic of the mechanical components during muscle relaxation is still unknown.

One of the most studied paradigms capable to induce alterations in stiffness is static stretching (SS). SS-induced alterations in muscle-tendon unit, muscle and tendon stiffness have been observed [17–19]. A prior study reported lengthening in components of delay during electrically evoked contraction after SS [14]. However, if such variations would also occur after SS during relaxation at different joint angles still remains an open question.

Therefore, the aim of the study was twofold: (1) to assess the changes in components of  $R\text{-Delay}_{\text{TOT}}$  after electrically evoked contractions at different joint angles; and (2) to assess the influence of SS on these components at the same joint angles.

## Methods

### Participants

Nineteen physically active males (mean  $\pm$  standard deviation: age  $24 \pm 3$  years; body mass  $76.4 \pm 8.9$  kg; stature  $1.78 \pm 0.09$  m; *gastrocnemius medialis* (GM) skinfold  $7.8 \pm 1.3$  mm; *gastrocnemius lateralis* skinfold  $5.1 \pm 1.2$  mm; calf circumference  $37.9 \pm 3.3$  cm) volunteered for this study. After receiving a full explanation of the experimental procedures, each participant gave a written informed consent. Participants were all clinically healthy with no previous history of lower limb injuries. They were asked to abstain from caffeine or ergogenic beverages in the 24 h preceding the test and to report to the laboratory without any form of physical exercise of heavy intensity in the previous 48 h. The study was approved by the local university ethical committee and performed in accordance with the principles of the 1975 Declaration of Helsinki.

### Experimental protocol

A schematic drawing of the time course of the tests is given in Fig. 1. After a first visit for familiarization purposes,

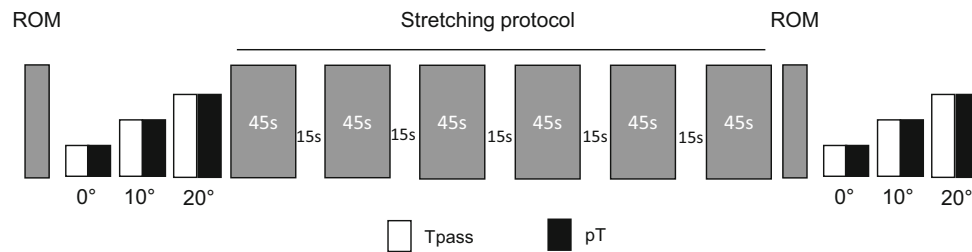


**Fig. 1** Experimental design: range of motion (ROM), plantar flexor muscles passive torque ( $T_{pass}$ ) and electrically evoked contraction torque (3 s at 50 Hz stimulation,  $pT$ ) were measured before and after application of static stretching (six elongations of 45 s with 15 s of

rest in between).  $T_{pass}$  and  $pT$  were measured at 0°, 10°, and 20° of dorsiflexion. Measurements were performed twice for intra-session reliability assessment

participants reported to the laboratory a second day for testing procedures. All experiments were carried out in a room at constant temperature ( $22 \pm 1$  °C) and relative humidity ( $50 \pm 5$  %). During tests, participants laid prone on a custom-made ergometer with a mobile metal plate connected to a previously calibrated load cell (mod. SM-2000 N, Interface, UK; operating linearly between 0 and 2000 N). The ankle of the dominant limb was firmly attached to the mobile metal plate by inelastic strap to minimize heel displacement. Hip and shoulders were firmly secured to the ergometer. The load cell was kept in line with the direction of force output. A bi-axial electrogoniometer (mod. TSD 130A, Biopac System, CA, USA) was positioned on the external face of the fibula and on the calcaneum to calculate ankle range of motion (ROM).

After ROM assessment (about 15 s), the foot was positioned at 0° (corresponding with the perpendicularity of the tibia relative to the longitudinal axis of the foot), 10° and 20° of dorsiflexion to determine passive and maximum electrically evoked peak force at each angle. The EMG, MMG and force signals were recorded during contractions. The same procedure was followed immediately after SS, without removing the stimulation and EMG electrodes.

**Stretching intervention** SS was administered manually by the same operator while the participant laid prone on the ergometer, with the ankle attached to the metal plate. SS consisted of six elongations (45 s each with in-between rest of 15 s) of the plantar flexor muscles up to the point of discomfort, starting with the foot in a relaxed position (about  $-20^\circ$  of dorsiflexion) [12, 20–24]. To avoid reflex activation, the muscles were stretched in about 3 s, with participants keeping the stretched muscles as relaxed as possible. EMG signal was constantly monitored during SS to check for any reflex muscle activity.

**ROM** The ankle joint ROM was determined starting with the ankle at its resting position (about  $-20^\circ$  of dorsiflexion) and manually dorsiflexed at slow speed, up to participant's point of discomfort. The same procedure was followed after SS, always starting from the resting position previously determined.

**Force, EMG and MMG signals** The passive force exerted by plantar flexor muscles against the ergometer platform was recorded at 0°, 10° and 20° of dorsiflexion and the peak force elicited by a tetanic stimulation (3 s at 50 Hz, amperage range: 10–100 mA; pulse duration: 304  $\mu$ s, stimulation amplitude: +10 % of the maximum compound motor action potential) was measured at the same joint angles separated by 5 min of rest in between. The tibial nerve was supramaximally stimulated by an electrical stimulator (mod. St-Pro Multichannel Programmable Neuromuscular Stimulator, LiSin, Turin, Italy). The receiving electrode ( $70 \times 35$  mm) was positioned perpendicularly on the upper margin of the patella, whereas the stimulating electrode ( $35 \times 35$  mm) was placed above the tibial nerve at the popliteal fossa level. Force signal was acquired by a data acquisition system (mod. UM150, Biopac System, Santa Barbara, USA) and driven to the auxiliary input of the EMG amplifier (mod. EMG-USB, OT Bioelettronica, Turin, Italy).

Surface EMG and MMG signals were detected by an integrated probe, which included four silver bars electrodes (width 1 mm, length 10 mm, inter-electrode distance 10 mm) for differential EMG detection (mod. ELSCH004, diameter 1 mm, length 10 mm, inter-electrode distance 10 mm, OT Bioelettronica, Turin, Italy), and a mono-directional accelerometer (mod. ADXL202JE, Analog Devices, Norwood, MA, USA) placed between the first and second electrode, providing the MMG signal. The skin area under the EMG electrodes was gently abraded with fine sand paper, cleaned carefully with ethyl alcohol, and prepared with a conductive cream (Nuprep, Weaver and Co., Aurora, USA) to achieve inter-electrode impedance below 2000  $\Omega$ . The integrated probe was placed over the GM muscle belly along muscle fiber direction, with the EMG electrodes positioned perpendicularly to the major axes of the fibers between the tendon and the motor point, in accordance with the European recommendations for surface EMG [25]. The accelerometer was positioned in proximity to the point of maximum skin displacement during contraction. The probe was then fixed steadily by an

adhesive elastic band (Fixomull Stretch, Beiersdorf, Hamburg, Germany). EMG and MMG were amplified, filtered (bandwidth of 10–500 Hz and 4–120 Hz, respectively) and stored on a personal computer after A/D conversion (mod. EMG-USB, OT Bioelettronica, Turin, Italy), with a sampling rate of 10 kHz.

**Joint stiffness** Joint stiffness was calculated from the passive torque-angle curve fitted with a second-order polynomial regression model [26]. The slope of the curve at 0°, 10°, and 20° of dorsiflexion was used as measure of joint stiffness. Previous studies presented very high intra-class correlation coefficient (ICC, range: 0.902–0.934) and a small standard error of measurement as percentage (SEM%, range 2.4–5.1 %) for stiffness calculation [17, 19].

### Data analysis

The passive force was calculated as the average of the force signal recorded during the first 5 s after ankle positioning. The peak force during electrically evoked contraction was identified as the highest level of force achieved during the tetanic stimulations. Torque was calculated by multiplying the force output for the distance between the external malleolus and the force application point. The passive torque ( $T_{pass}$ ) and peak torque (pT) were then defined.

EMG was analyzed in time and frequency domain: the root mean square (RMS) and mean frequency (MF) of the signals were calculated from epochs of 1 s, corresponding to the central part of the force plateau reached during each contraction of 3 s.

From the MMG signal, the maximum MMG amplitude of the relaxation phase (R-MMG<sub>p-p</sub>) and the RMS from epochs of the same time window used for EMG RMS calculation were determined at each angle.

The force, EMG and MMG parameters, which were calculated with a similar set-up, presented an ICC ranging from 0.908 to 0.994 and SEM% ranging from 1.0 to 3.7 % [17, 19].

According to previous investigations [7, 8], R-Delay<sub>TOT</sub> was divided in: (1) R-Δt EMG-F, from EMG offset to F decay onset; (2) R-Δt F-MMG<sub>p-p</sub>, from F decay onset to the beginning of the R-MMG<sub>p-p</sub>; (3) R-Δt MMG<sub>p-p</sub>, from the beginning to the end of R-MMG<sub>p-p</sub>; and (4) R-Δt MMG-F<sub>end</sub>, from the end of R-MMG<sub>p-p</sub> to F return toward baseline. To exclude possible sources of error due to signal artifacts, delays' detection was confirmed by an expert operator through visual inspection. Data analysis was performed by a custom-built routine using a commercially available software (Labview 7.1. National Instruments, Austin, TX, USA). A representative image of signals calculation in one participant is given in Fig. 2.

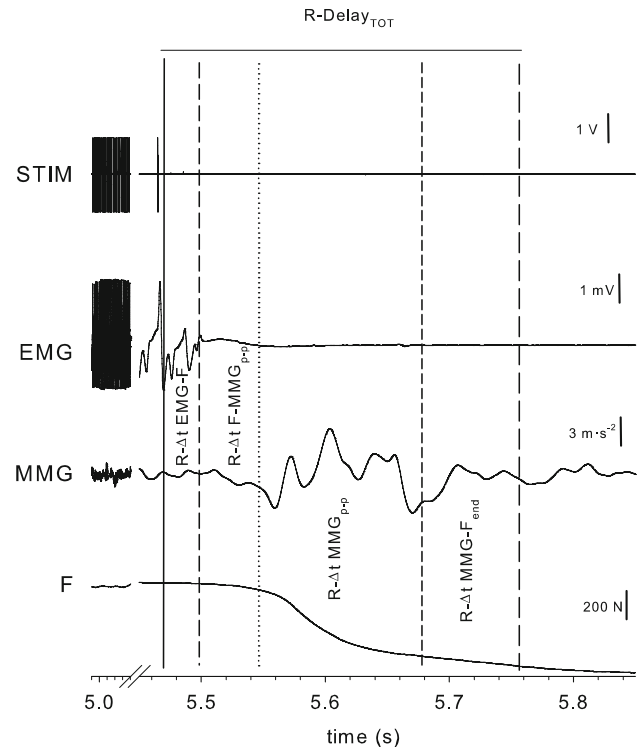


**Fig. 2** Current stimulation (Stim), electromyogram (EMG), mechanomyogram (MMG) and force (F) signals and delays in a representative participant. The *solid, dashed, dotted, short dashed and long dashed lines* indicate the negative peak of EMG signal, the initial decrease in F signal, the beginning of the maximum displacement of the MMG signal (MMG<sub>p-p</sub>), the duration of MMG<sub>p-p</sub> and the return of F signal at baseline, respectively. For delays explanation, see “Methods”

### Statistical analysis

The normal distribution of the data was checked by the Shapiro–Wilk’s test. A sample size of nineteen participants was selected to ensure a statistical power >0.80. Pre- and post-SS differences in ROM were assessed by a paired Student’s *t* test. SS-induced effects on all the other parameters were determined by a two-way (time × joint angle) analysis of variance (ANOVA) for repeated measures, with a Holm-Sidak post-hoc test when necessary. Changes magnitude was determined using effect size (ES) statistics, with the standard error of ES estimate [27], or partial eta squared ( $\eta_p^2$ ) when appropriate [28]. ES was classified as trivial (<0.2), small (0.2–0.6), moderate (0.6–1.2), large (1.2–2.0), and very large when >2.0 [27]. A two-way, mixed model ICC and SEM% assessed intra-session reliability for delays measurements. ICC values were considered as very high >0.90, high (0.70–0.89), and moderate (0.50–0.69) [29]. The minimum detectable change at 95 % confidence as a percentage (MDC<sub>95%</sub>) assessed the sensitivity of the parameters in detecting stretch-induced changes [30, 31]. Results are

expressed as mean±standard error (SE). Data were analyzed using SPSS® Statistics (v. 22, Armonk, NY, USA).

### Results

The ICC and SEM% for delays values are provided in Table 1. According to our categories (see “Methods”), delays presented from high to very high intra-session reliability, with ICC ranging from 0.87 to 0.92, and SEM% ranging from 1.1 to 2.6 % of the relative mean value. All delays presented a relative change between pre- and post-SS higher than those required by MDC<sub>95%</sub>.

Both pre- and post-SS  $T_{pass}$  (Fig. 3a) increased significantly with the joint angle ( $P < 0.001$ ,  $\eta_p^2 = 0.842$ ). After SS,  $T_{pass}$  decreased significantly at all the investigated joint angles. Decrements ranged from 27 % at 0° to 23 % at 20° ( $P < 0.001$ ,  $\eta_p^2 = 0.494$ ). A significant interaction between the two factors (time × joint angle) was found ( $P = 0.003$ ,  $\eta_p^2 = 0.510$ ).

Similarly, joint stiffness (Fig. 3b) increased significantly with the angle ( $P < 0.001$ ,  $\eta_p^2 = 0.741$ ). After SS, joint stiffness decreased significantly at all angles, with decrement ranging from 16 % at 0° to 20 % at 20° ( $P < 0.001$ ,  $\eta_p^2 = 0.552$ ). A significant interaction between the two factors (time × joint angle) was found ( $P = 0.002$ ,  $\eta_p^2 = 0.591$ ).

As expected, SS increased significantly the ankle ROM from  $43 \pm 1^\circ$  to  $50 \pm 2^\circ$  ( $P < 0.001$ ; ES  $0.85 \pm 0.39$ ).

The changes in pT, EMG RMS, EMG MF, are given in Fig. 4. After SS, pT (Fig. 4a) decreased significantly at all joint angles (from 11 to 13 %,  $P < 0.001$ ,  $\eta_p^2 = 0.580$ ), while EMG RMS and MF (Fig. 4b, c, respectively) were similar to their pre-stretching values ( $P > 0.05$ ).

The average duration of R-Delay<sub>TOT</sub> and its components is reported in Fig. 5. Before SS, R-Delay<sub>TOT</sub> and its mainly

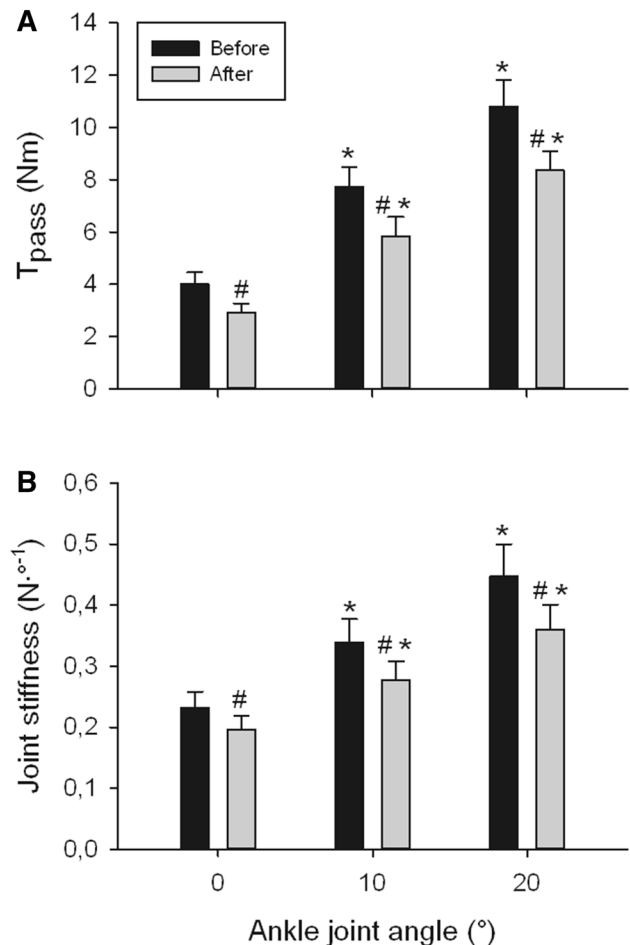


**Fig. 3** Changes in  $T_{pass}$  (a) and joint stiffness (b) at the different ankle joint angles, before (black bars) and after (gray bars) static stretching. \* $P < 0.05$  vs 0°; # $P < 0.05$  vs before.  $T_{pass}$  passive torque

mechanical components decreased significantly with the increase in dorsiflexion angle (decrement range 5–25 %,  $P < 0.05$ ). After SS, all components of R-Delay<sub>TOT</sub>

**Table 1** Intrasection reliability and sensitivity of measurements between trials 1 and 2

Delay (ms)	Trial 1 ( $m \pm SD$ )	Trial 2 ( $m \pm SD$ )	ICC	SEM%	MDC <sub>95%</sub>	Measured changes (95 % CI)
R-Δt EMG-F	26.1 ± 3.2	26.4 ± 3.1	0.92	2.0	3.9	12.4 (10.4–14.3)
R-Δt F-MMG <sub>p-p</sub>	53.0 ± 2.5	52.9 ± 2.2	0.91	2.5	4.9	28.5 (26.6–30.5)
R-Δt MMG <sub>p-p</sub>	90.7 ± 7.6	91.3 ± 6.8	0.88	2.6	5.2	19.1 (17.2–21.1)
R-Δt MMG-F <sub>end</sub>	78.8 ± 8.0	77.5 ± 8.3	0.87	2.4	4.7	17.7 (15.8–19.7)
R-Delay <sub>TOT</sub>	259.1 ± 9.6	261.5 ± 9.1	0.88	1.1	2.2	20.0 (17.8–21.7)

The intraclass correlation coefficient (ICC), standard error of measurements as a percentage (SEM%), minimal detectable change at 95 % confidence as a percentage (MDC<sub>95%</sub>) and the percentage difference between pre- and post-stretching values, with the lower and upper boundaries of the 95 % confidence interval (CI) are reported for each delay

*m* mean, *SD* standard deviation, *EMG* electromyogram, *MMG* mechanomyogram, *F* force, *R-tΔ EMG-F* time delay between muscle electrical activation cessation and the beginning of force decay, *R-Δt F-MMG<sub>p-p</sub>* time delay between force decay beginning and the largest MMG signal displacement during relaxation, *R-Δt MMG<sub>p-p</sub>* duration of peak-to-peak of the largest MMG signal displacement during relaxation, *R-Δt MMG-F<sub>end</sub>* time delay between the largest MMG displacement and force cessation, *R-Delay<sub>TOT</sub>* total relaxation delay

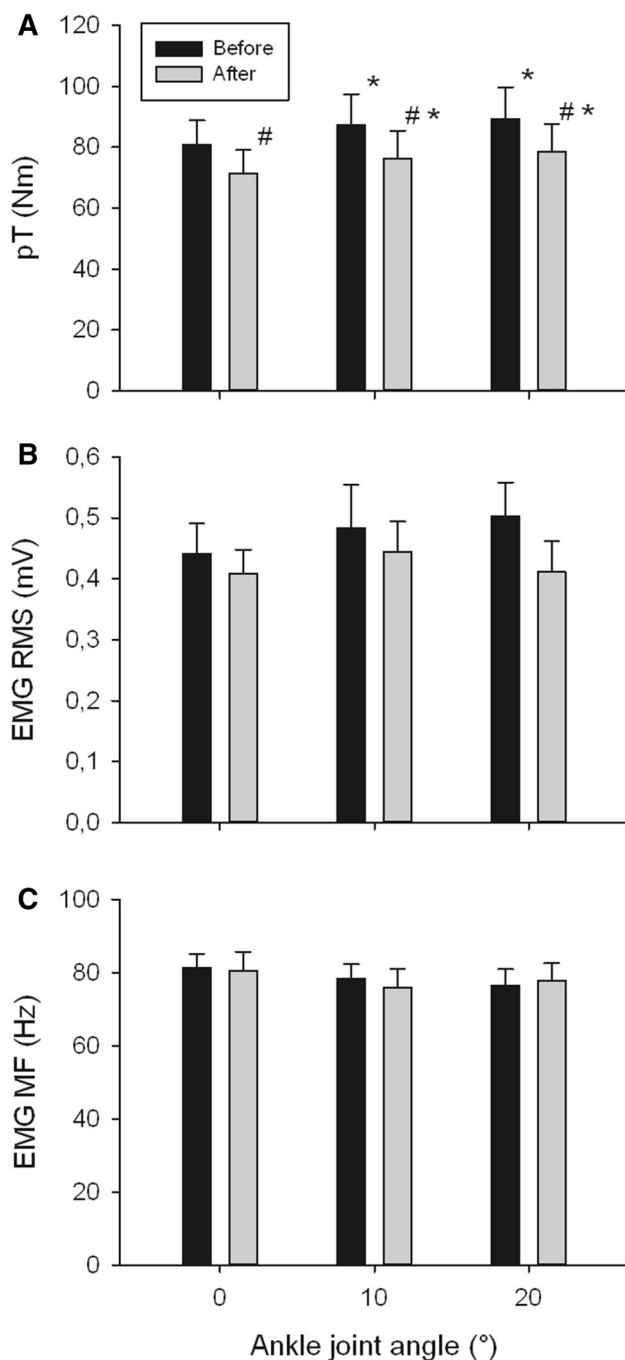


**Fig. 4** pT (a), EMG RMS (b), and MF (c) at the different ankle joint angles, before (black bars) and after (gray bars) static stretching. \* $P < 0.05$  vs 0°; # $P < 0.05$  vs before. pT peak torque, EMG RMS electromyogram root mean square, EMG MF electromyogram mean frequency

lengthened significantly (increment range 14–25 %,  $P < 0.05$ ,  $\eta_p^2$  ranging from 0.309 to 0.603 at the different joint angles). These delays decreased significantly with the increments in dorsiflexion angle (decrease range 22–45 %,  $P < 0.05$ ) also after SS.

## Discussion

The main findings of the present study were that: (1) the main mechanical components of R-Delay<sub>TOT</sub> decreased with an increase in joint angle both before and after SS; and (2) passive stretching significantly increased all the components of R-Delay<sub>TOT</sub>.

The very high ICC values found in all measurements indicate that this EMG, MMG and force combined approach can provide reliable delay measurements. The significant stretch-induced changes in R-Delay<sub>TOT</sub> and its components above the MDC<sub>95%</sub> indicate that this means can also offer adequate levels of sensitivity. These data are in line with previous studies [7–9], confirming the notion that this combined approach can be applied to evaluate delays changes under different experimental conditions.

As previously reported [20, 32, 33], stretching did not affect EMG characteristics (RMS and MF) during electrically evoked contractions. Thus, the present EMG results confirm that neuromuscular synapsis efficiency and sarcolemmal action potential propagation of the contracting muscle were unaffected by stretching.

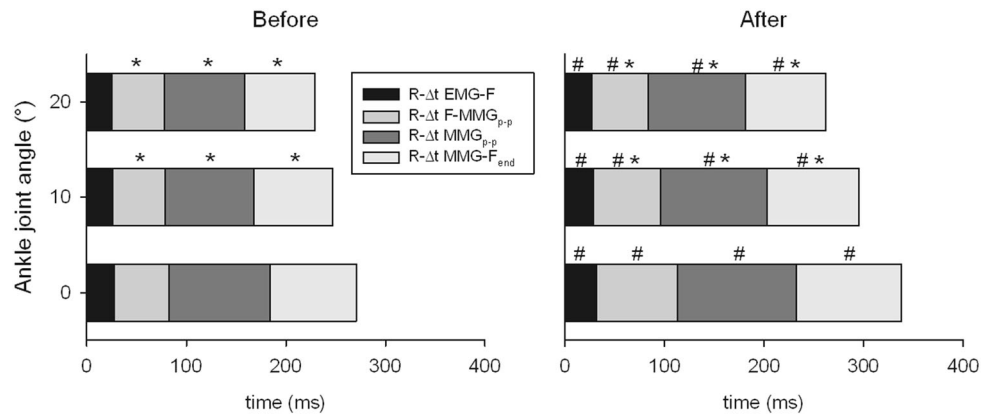
Before SS, R-Delay<sub>TOT</sub> decreased with the increase of the dorsiflexion angle because of a decrease in the three mainly mechanical but not in the mainly electrochemical component. Interestingly, this reduction was observed also after SS. These findings agree with a prior study, showing similar results during the contraction phase in the biceps brachii muscle [15]. Such a decrease was suggested to be the result of a reduction in muscle-tendon unit slack occurring when the muscle is contracted starting from a length longer than that at rest. This was likely the case also during muscle relaxation. The higher passive torque reached at 20° of dorsiflexion may have enhanced the speed at which sarcomeres and SEC returned to the starting point after an electrically evoked contraction.

## Delays after stretching

In line with prior works [14, 20, 33–35], SS-induced a decrease in pT. This reduction is usually ascribed to changes in neuromuscular factors, such as a reduction in neural drive from the central nervous system to the muscle [21–24, 32, 35–37], and stretching-induced mechanical alterations, among which a reduction in muscle-tendon unit stiffness [17–19]. In the present study electrically evoked contractions were used, therefore the reduction in maximum torque should be mainly explained by mechanical alterations.

After stretching, R-Delay<sub>TOT</sub> increased significantly by about 20 %. All the components contributed to R-Delay<sub>TOT</sub> lengthening, with a larger role played by the mechanical

**Fig. 5** Total electromechanical delay during relaxation (R-Delay<sub>TOT</sub>) components duration before and after static stretching. \* $P < 0.05$  vs 0°; # $P < 0.05$  vs before. For delays explanation, see “Methods”



parts. The increase in the whole electromechanical latency during contraction after stretching was previously observed [14, 38]. However, to the best of our knowledge, no studies focused on the calculation of the electromechanical delay during muscle relaxation; therefore, comparisons with the literature cannot be done.

After stretching R-Δt EMG-F lengthened by about 12 %. To explain such a change, it may be hypothesized an increase in Ca<sup>2+</sup> sensitivity at longer sarcomere's length [39], a condition that can likely reflect the post-stretching sarcomeres state. This mechanism could delay the transition of cross-bridges from force-generating to non-force-generating status, thus increasing the mainly electrochemical latency.

All the mechanical components were significantly longer after SS, in particular R-Δt F-MMG<sub>p-p</sub>. During muscle relaxation, the changes in joint stiffness found in the present study may have slowed cross-bridge and SEC dynamics, thus delaying the return of sarcomeres and SEC to their pre-contraction length.

## Conclusion

Our results suggest that, in the human GM muscle, the reduction in R-Delay<sub>TOT</sub> with the increase in dorsiflexion angle could be mainly ascribed to the increase in joint stiffness and not to alterations of the electrochemical processes during muscle relaxation. SS lengthened R-Delay<sub>TOT</sub> and all its components with a concomitant decrease in joint stiffness. Nevertheless, the reduction in the main mechanical components of R-Delay<sub>TOT</sub> seen with the increase in dorsiflexion angle was similar to that observed before SS administration.

**Acknowledgments** The authors wish to thank all the participants involved in the study, for their patience and committed involvement. The study was supported by a PUR Grant 2008 (#12-1-5059-281-10) assigned to Fabio Esposito by the Università degli Studi di Milano.

## Compliance with ethical standards

**Conflict of interest** The authors declare that they have no conflict of interest.

**Ethical approval** All procedures performed in studies involving human participants were in accordance with the ethical Standards of the institutional or national research committee and with the 1964 Helsinki declaration and its later amendments or compatible ethical Standards. This article does not contain any studies with animals performed by any of the authors.

**Informed consent** Informed consent was obtained from all individual participants included in this study.

## References

- Viitasalo JT, Komi PV (1981) Interrelationships between electromyographic, mechanical, muscle structure and reflex time measurements in man. *Acta Physiol Scand* 111:97–103
- Blanpied P, Oksendahl H (2006) Reaction times and electromechanical delay in reactions of increasing and decreasing force. *Percept Mot Ski* 103:743–754
- Corsier T (1974) Temporal discrepancies in the electromyographic study of rapid movement. *Ergonomics* 17:389–400. doi:10.1080/00140137408931362
- Ferris-Hood K, Threlkeld AJ, Horn TS, Shapiro R (1996) Relaxation electromechanical delay of the quadriceps during selected movement velocities. *Electromyogr Clin Neurophysiol* 36:157–170
- Miyashita M, Miura M, Matsui H, Minamitate K (1972) Measurement of the reaction time of muscular relaxation. *Ergonomics* 15:555–562. doi:10.1080/00140137208924457
- Vos EJ, Mullender MG, van Ingen Schenau GJ (1990) Electromechanical delay in the vastus lateralis muscle during dynamic isometric contractions. *Eur J Appl Physiol Occup Physiol* 60:467–471
- Cè E, Rampichini S, Venturelli M et al (2014) Electromechanical delay components during relaxation after voluntary contraction: reliability and effects of fatigue. *Muscle Nerve*. doi:10.1002/mus.24466
- Esposito F, Cè E, Rampichini S et al (2016) Electromechanical delay components during skeletal muscle contraction and relaxation in patients with myotonic dystrophy type 1. *Neuromuscul Disord* 26:60–72. doi:10.1016/j.nmd.2015.09.013

9. Cè E, Rampichini S, Limonta E, Esposito F (2014) Fatigue effects on the electromechanical delay components during the relaxation phase after isometric contraction. *Acta Physiol*. doi:[10.1111/apha.12212](https://doi.org/10.1111/apha.12212)
10. Cè E, Rampichini S, Esposito F (2015) Novel insights into skeletal muscle function by mechanomyography: from the laboratory to the field. *Sport Sci Health* 11:1–28. doi:[10.1007/s11332-015-0219-z](https://doi.org/10.1007/s11332-015-0219-z)
11. Rampichini S, Cè E, Limonta E, Esposito F (2014) Effects of fatigue on the electromechanical delay components in gastrocnemius medialis muscle. *Eur J Appl Physiol* 114:639–651. doi:[10.1007/s00421-013-2790-9](https://doi.org/10.1007/s00421-013-2790-9)
12. Cè E, Rampichini S, Limonta E, Esposito F (2013) Torque and mechanomyogram correlations during muscle relaxation: effects of fatigue and time-course of recovery. *J Electromyogr Kinesiol* 23:1295–1303. doi:[10.1016/j.jelekin.2013.09.007](https://doi.org/10.1016/j.jelekin.2013.09.007)
13. Cè E, Rampichini S, Agnello L et al (2013) Effects of temperature and fatigue on the electromechanical delay components. *Muscle Nerve* 47:566–576. doi:[10.1002/mus.23627](https://doi.org/10.1002/mus.23627)
14. Esposito F, Limonta E, Cè E (2011) Passive stretching effects on electromechanical delay and time course of recovery in human skeletal muscle: new insights from an electromyographic and mechanomyographic combined approach. *Eur J Appl Physiol* 111:485–495. doi:[10.1007/s00421-010-1659-4](https://doi.org/10.1007/s00421-010-1659-4)
15. Sasaki K, Sasaki T, Ishii N (2011) Acceleration and force reveal different mechanisms of electromechanical delay. *Med Sci Sport Exerc* 43:1200–1206. doi:[10.1249/MSS.0b013e318209312c](https://doi.org/10.1249/MSS.0b013e318209312c)
16. Muraoka T, Muramatsu T, Fukunaga T, Kanehisa H (2004) Influence of tendon slack on electromechanical delay in the human medial gastrocnemius in vivo. *J Appl Physiol* 96:540–544. doi:[10.1152/jappphysiol.01015.2002](https://doi.org/10.1152/jappphysiol.01015.2002)
17. Longo S, Cè E, Rampichini S et al (2014) Mechanomyogram amplitude correlates with human gastrocnemius medialis muscle and tendon stiffness both before and after acute passive stretching. *Exp Physiol* 99:1359–1369. doi:[10.1113/expphysiol.2014.080366](https://doi.org/10.1113/expphysiol.2014.080366)
18. Morse CI, Degens H, Seynnes OR et al (2008) The acute effect of stretching on the passive stiffness of the human gastrocnemius muscle tendon unit. *J Physiol* 586:97–106
19. Cè E, Longo S, Rampichini S et al (2015) Stretch-induced changes in tension generation process and stiffness are not accompanied by alterations in muscle architecture of the middle and distal portions of the two gastrocnemii. *J Electromyogr Kinesiol* 25:469–478. doi:[10.1016/j.jelekin.2015.03.001](https://doi.org/10.1016/j.jelekin.2015.03.001)
20. Cè E, Paracchino E, Esposito F (2008) Electrical and mechanical response of skeletal muscle to electrical stimulation after acute passive stretching in humans: a combined electromyographic and mechanomyographic approach. *J Sports Sci* 26:1567–1577. doi:[10.1080/02640410802277429](https://doi.org/10.1080/02640410802277429)
21. Limonta E, Cè E, Esposito F (2012) Effects of acute passive stretching on ventilatory pattern during prolonged cycle exercise. *Sport Sci Health* 7:105–110. doi:[10.1007/s11332-012-0122-9](https://doi.org/10.1007/s11332-012-0122-9)
22. Limonta E, Cè E, Rampichini S et al (2013) Effects of acute passive stretching on mean response time during an incremental ramp test. *Sport Sci Health* 9:25–30. doi:[10.1007/s11332-013-0141-1](https://doi.org/10.1007/s11332-013-0141-1)
23. Esposito F, Cè E, Limonta E (2012) Cycling efficiency and time to exhaustion are reduced after acute passive stretching administration. *Scand J Med Sci Sports* 22:737–745. doi:[10.1111/j.1600-0838.2011.01327.x](https://doi.org/10.1111/j.1600-0838.2011.01327.x)
24. La Torre A, Castagna C, Gervasoni E et al (2010) Acute effects of static stretching on squat jump performance at different knee starting angles. *J Strength Cond Res* 24:687–694. doi:[10.1519/JSC.0b013e3181c7b443](https://doi.org/10.1519/JSC.0b013e3181c7b443)
25. Hermens H, Freiks B, Merletti R et al (1999) European recommendations for surface electromyography. RRD, The Netherlands
26. Mizuno T, Matsumoto M, Umemura Y (2013) Decrements in stiffness are restored within 10 min. *Int J Sports Med* 34:484–490
27. Rhea MR (2004) Determining the magnitude of treatment effects in strength training research through the use of the effect size. *J Strength Cond Res* 18:918. doi:[10.1519/14403.1](https://doi.org/10.1519/14403.1)
28. Cohen J (1988) *Statistical power analysis for the behavioral sciences*, 2nd edn. Lawrence Erlbaum Associates, Mahwah
29. Munro BH (2004) *Statistical methods for health care research*, 5th edn. Lippincott William and Wilkins, Philadelphia
30. Tesio L, Longo S, Rota V (2011) The subjective visual vertical: validation of a simple test. *Int J Rehabil Res* 34:307–315. doi:[10.1097/MRR.0b013e32834c45bc](https://doi.org/10.1097/MRR.0b013e32834c45bc)
31. Tesio L, Rota V, Longo S, Grzeda MT (2013) Measuring standing balance in adults: reliability and minimal real difference of 14 instrumental measures. *Int J Rehabil Res* 36:362–374. doi:[10.1097/MRR.0000000000000037](https://doi.org/10.1097/MRR.0000000000000037)
32. Cè E, Rampichini S, Maggioni MA et al (2008) Effects of passive stretching on post-activation potentiation and fibre conduction velocity of biceps brachii muscle. *Sport Sci Health* 4:43–50. doi:[10.1007/s11332-008-0066-2](https://doi.org/10.1007/s11332-008-0066-2)
33. Esposito F, Limonta E, Cè E (2011) Time course of stretching-induced changes in mechanomyogram and force characteristics. *J Electromyogr Kinesiol* 21:795–802. doi:[10.1016/j.jelekin.2011.07.012](https://doi.org/10.1016/j.jelekin.2011.07.012)
34. Esposito F, Ce E, Rampichini S, Veicsteinas A (2009) Acute passive stretching in a previously fatigued muscle: electrical and mechanical response during tetanic stimulation. *J Sport Sci* 27:1347–1357. doi:[10.1080/02640410903165093](https://doi.org/10.1080/02640410903165093)
35. Cè E, Margonato V, Casasco M, Veicsteinas A (2008) Effects of stretching on maximal anaerobic power: the roles of active and passive warm-ups. *J Strength Cond Res* 22:794–800. doi:[10.1519/JSC.0b013e31816a4353](https://doi.org/10.1519/JSC.0b013e31816a4353)
36. Guissard N, Duchateau J, Hainaut K (1988) Muscle stretching and motoneuron excitability. *Eur J Appl Physiol Occup Physiol* 58:47–52
37. Cè E, Limonta E, Maggioni MA et al (2013) Stretching and deep and superficial massage do not influence blood lactate levels after heavy-intensity cycle exercise. *J Sports Sci* 31:856–866. doi:[10.1080/02640414.2012.753158](https://doi.org/10.1080/02640414.2012.753158)
38. Costa PB, Ryan ED, Herda TJ et al (2010) Acute effects of passive stretching on the electromechanical delay and evoked twitch properties. *Eur J Appl Physiol* 108:301–310. doi:[10.1007/s00421-009-1214-3](https://doi.org/10.1007/s00421-009-1214-3)
39. Claffin DR, Morgan DL, Julian FJ (1998) The effect of length on the relationship between tension and intracellular  $[Ca^{2+}]$  in intact frog skeletal muscle fibres. *J Physiol* 508(Pt 1):179–186